Atmospheric
Chemistry
and Physics
Discussions

Open Access

Supplement of

Observation of isoprene hydroxynitrates in the Southeastern United States and implications for the fate of NO$_x$

F. Xiong et al.

Correspondence to: P. B. Shepson (pshepson@purdue.edu)

1   CIMS calibration results for 4,3-IN

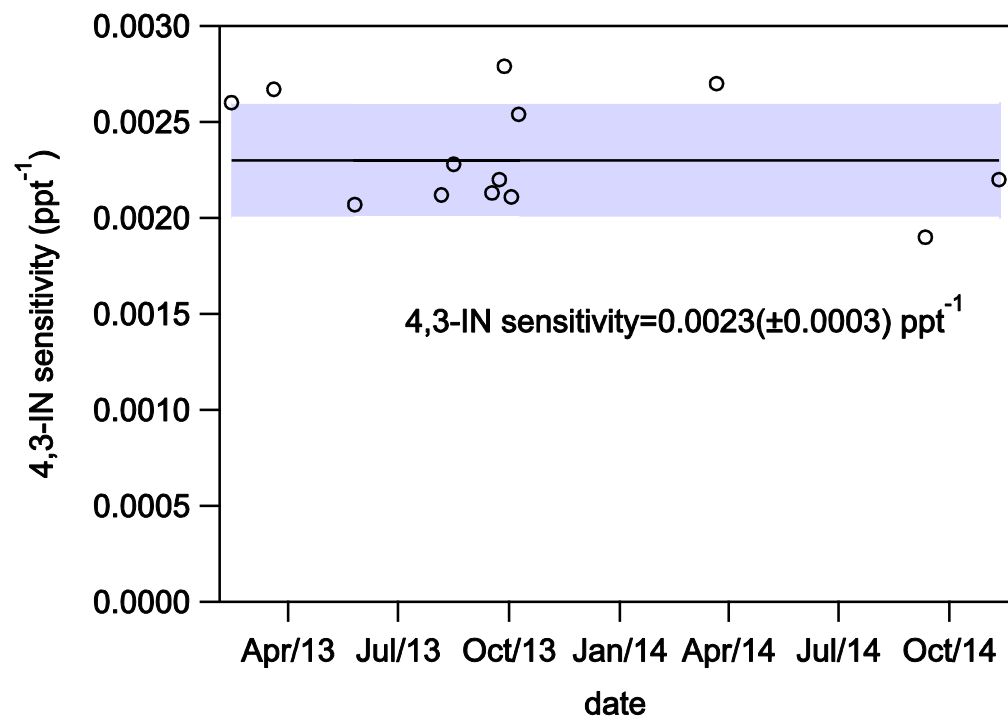Multiple CIMS calibrations for 4,3-IN have been conducted overtime, and the results were stable (Figure S1).

Figure S1. Calibration results for 4,3-IN. Each data point represents one calibration curve. The blue shade shows 1σ standard deviation of the measured sensitivity.

2   CIMS sensitivities for *cis*- and *trans*-1,4-IN

Three CIMS calibrations were conducted using standard solutions that contained a mixture of *cis*- and *trans*-1,4-IN. The relative abundance of the *cis* and *trans* isomers was determined from NMR spectra. The overall sensitivity and relative isomer abundance are listed in Table S1.

Table S1. Overall sensitivity and isomer composition for *cis*- and *trans*-1,4-IN calibration.

Calibration	Sensitivity (ppt^{-1})	Isomer composition (*trans* relative to *cis*)
1	$5.0(\pm0.5)\times10^{-4}$	3.4 ± 0.2
2	$5.0(\pm0.8)\times10^{-4}$	4.1 ± 0.3
3	$5.6(\pm0.8)\times10^{-4}$	3.4 ± 0.2

If we assume x is the sensitivity for *trans*-1,4-IN and y is the sensitivity for *cis*-1,4-IN, the isomer-weighted sensitivity measured by CIMS can be written as following.

$$0.77x+0.23y=5.0\times10^{-4} \tag{1}$$

$$0.80x+0.20y=5.0\times10^{-4} \tag{2}$$

$$0.77x+0.23y=5.6\times10^{-4} \tag{3}$$

Due to the uncertainties in the coefficients in equation (1) to (3), x and y in the above equation system cannot be solved. Therefore, we define function z through the following expression.

$$z=[5.0\times10^{-4}-(0.77x+0.23y)]^2+[5.0\times10^{-4}-(0.80x+0.20y)]^2+[5.6\times10^{-4}-(0.77x+0.23y)]^2 \tag{4}$$

The true values of x and y can be approximated by finding the minimum of z. Using this method, we calculate the sensitivity for *trans*-1,4-IN to be $3(\pm2)\times10^{-4} ppt^{-1}$ and the sensitivity for *cis*-1,4-IN to be $1.3(\pm0.3)\times10^{-3} ppt^{-1}$.

3   IN isomer distribution in chamber and field studies

3.1   Model simulation for chamber studies

An iterative method was used to determine the IN isomer distribution in chamber studies. The relative yield of the eight isoprene RO_2 radicals was used as the initial guess. The RO_2 isomeric distribution was calculated with the Kintecus simulation software (website http://www.kintecus.com/), based on the RO_2 interconversion and H-shift reaction rate constants proposed in the LIM1 mechanism (Peeters et al., 2014). An isomer-weighted IN sensitivity was derived from the calculated RO_2 isomer distribution. This sensitivity was used to calculate the initial guess value for the total IN yield (Figure S2).
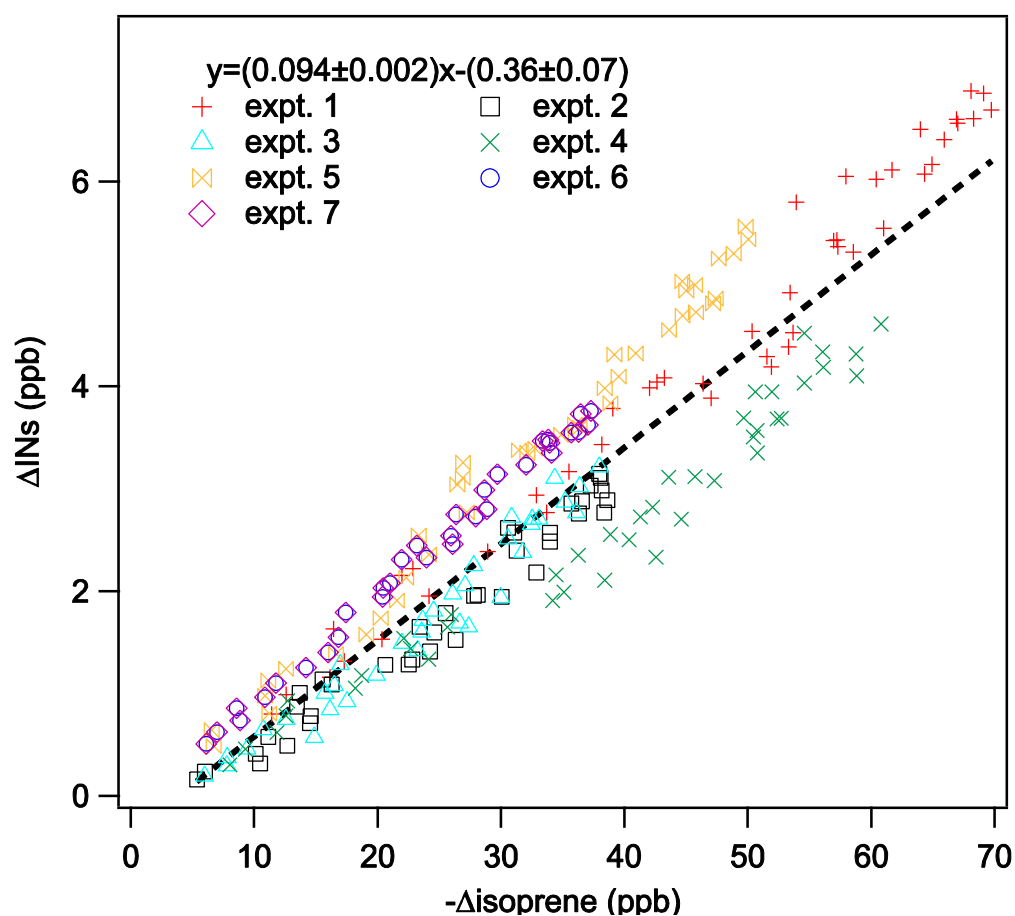

Figure S2. Initial guess value for IN yield, with IN sensitivity calculated based on RO_2 isomer distribution.

The iterative process was started by applying the guess value for IN yield in the MCM-based 0D model and simulating the production and loss of IN isomers in the chamber. From the model a time-dependent IN isomer distribution was obtained, which was then used to calculate the new isomer-weighted IN sensitivity and IN yield. The new IN yield was applied in the 0D model again, which generated an IN isomer distribution identical to the IN isomer distribution from which this new input IN yield was derived. Figure S3 shows the changing IN sensitivity derived from the 0D model.
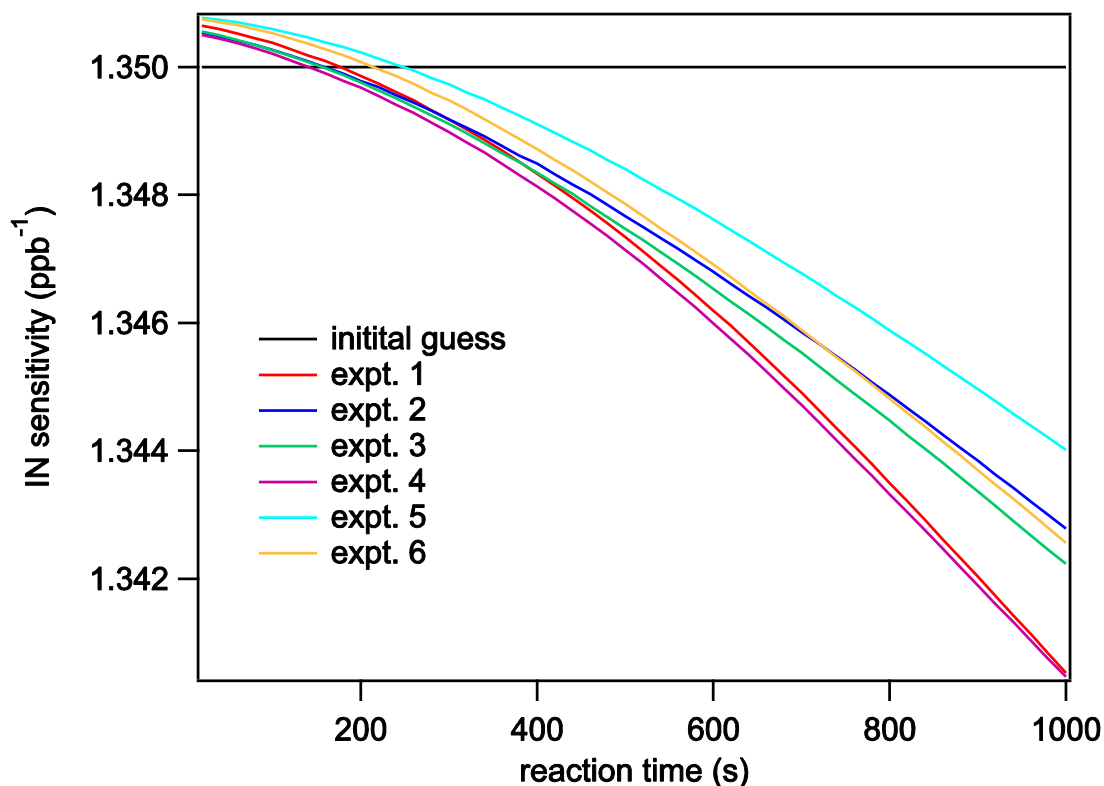

Figure S3. IN sensitivity with reaction time. The constant black line is the initial guess value derived from RO_2 isomer distribution. Only the first six experiments are shown, as the duration of the 7th experiment was 3600s and out of scale.

Figures S4~S7 show the model-observation comparison of isoprene, MVK+MACR, IN and NO for the chamber experiments. The red markers represent measurement data and the black markers represent model results. Each marker shape indicates one experiment.
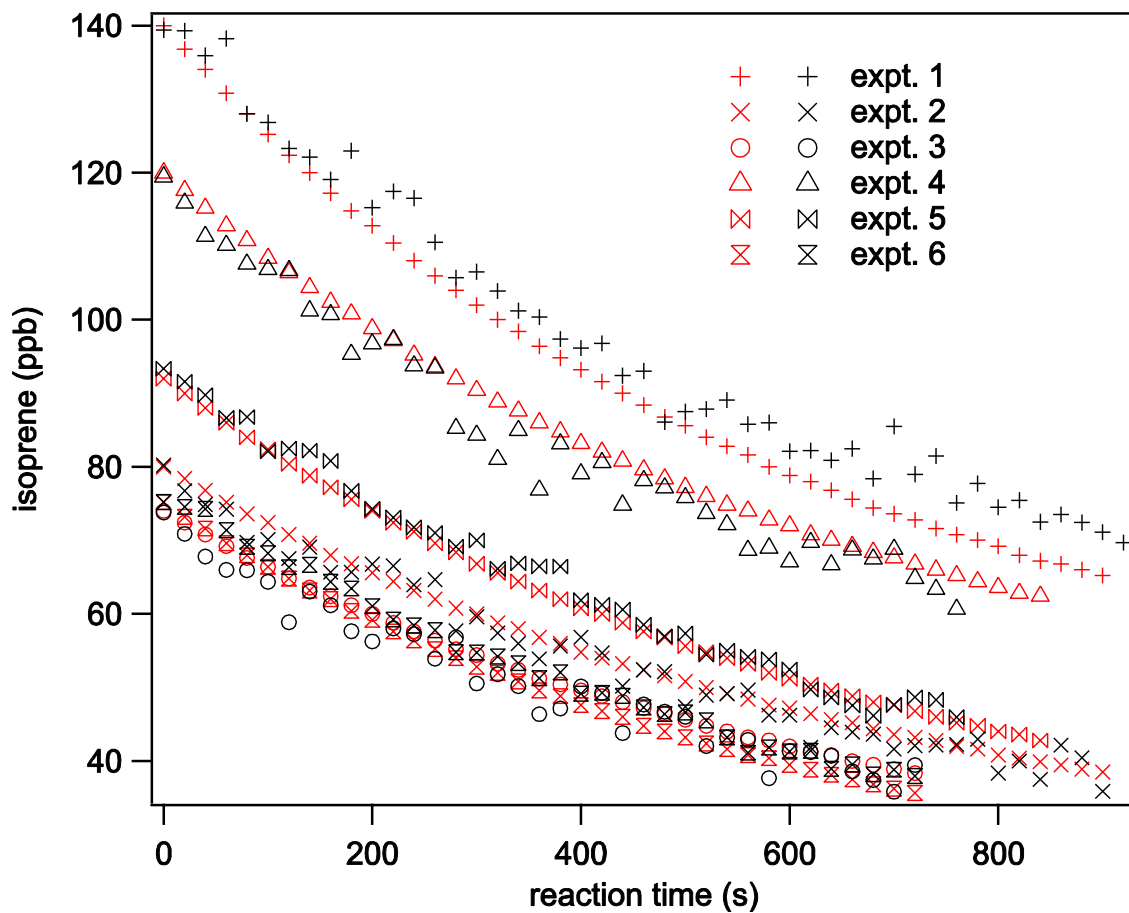
Figure S4. Model and measurement results of isoprene for chamber experiments. The red markers represent measurement data and the black markers represent model results.
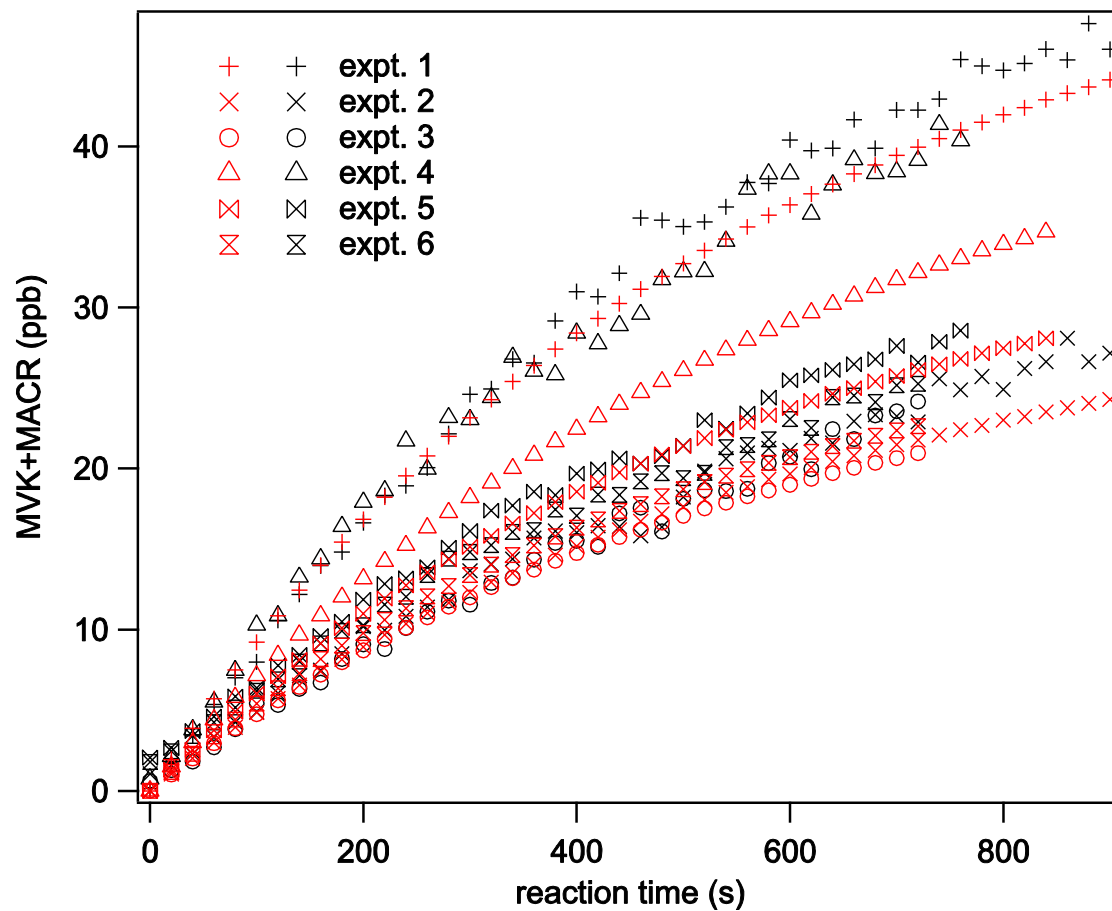
Figure S5. Model and measurement results of the sum of MVK and MACR for chamber experiments. The red markers represent measurement data and the black markers represent model results.
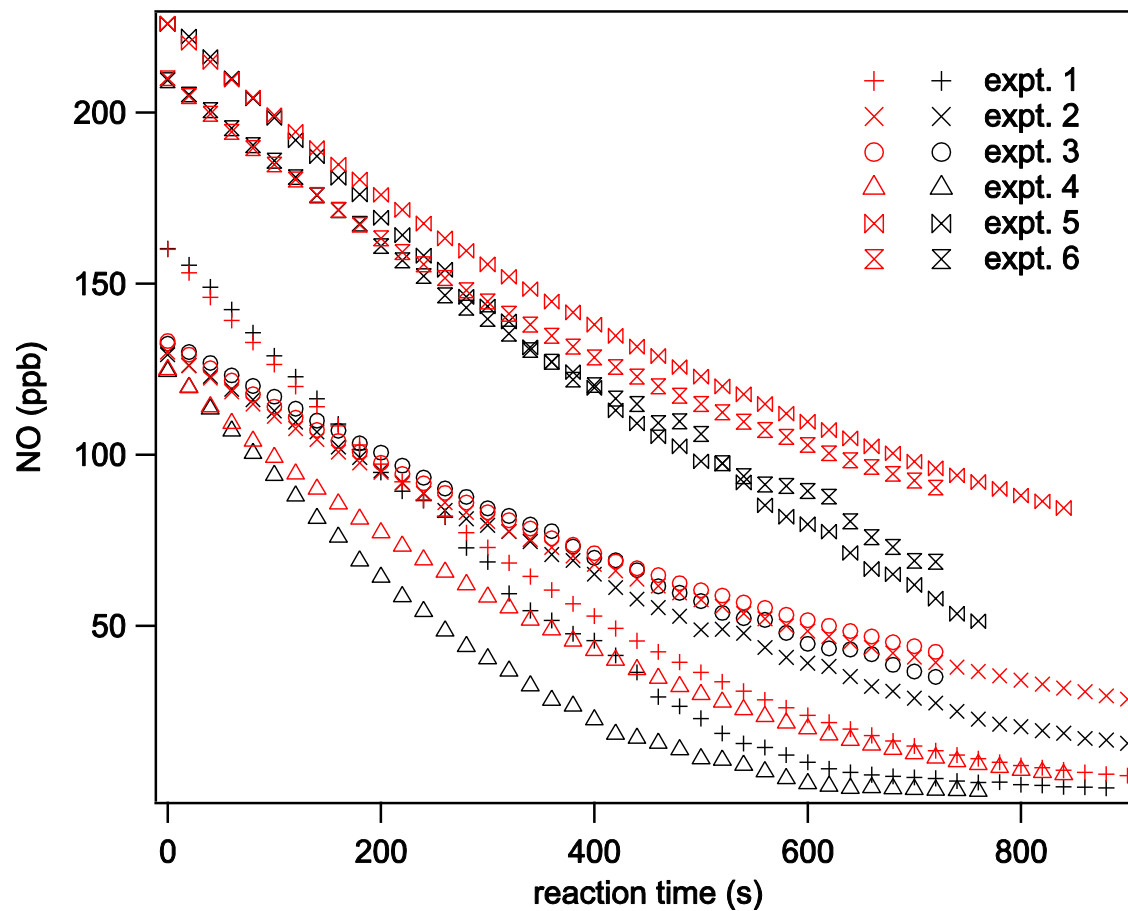
Figure S6. Model and measurement results of NO for chamber experiments. The red markers represent measurement data and the black markers represent model results. Each marker shape indicates one experiment.
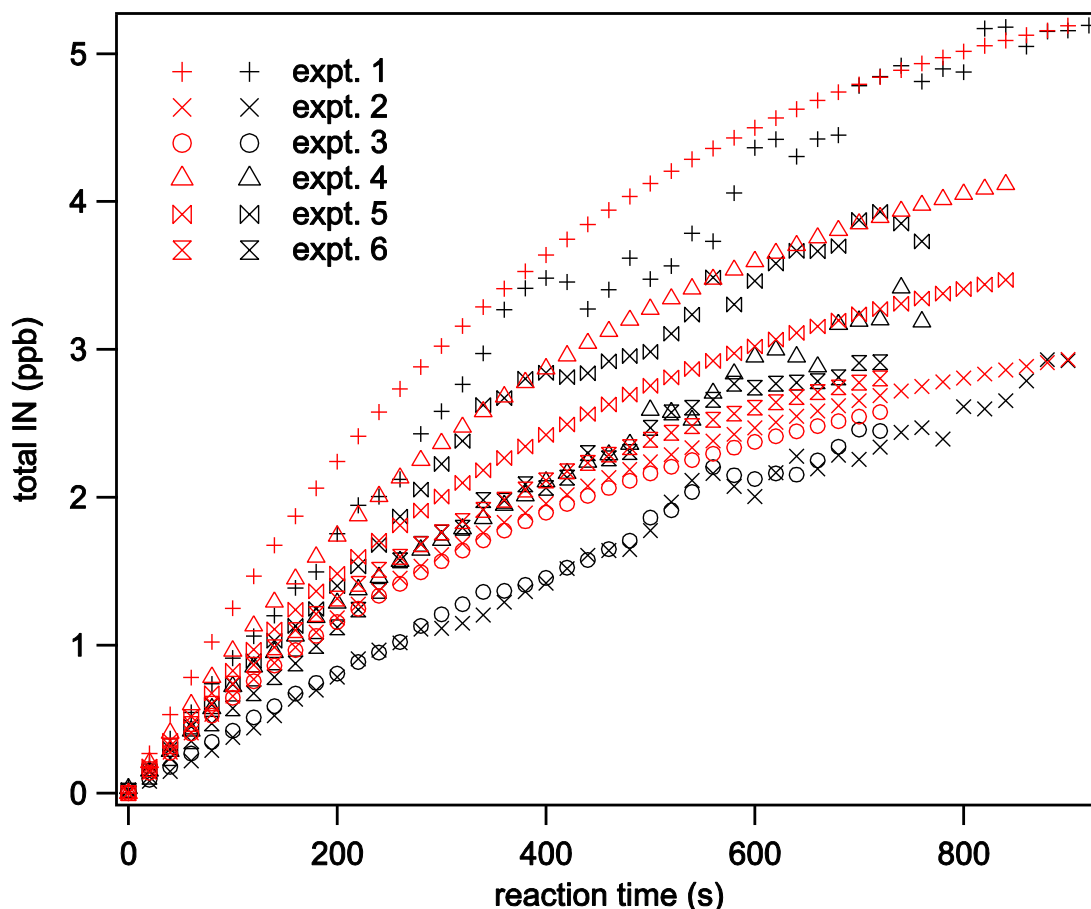
Figure S7. Model and measurement results of total IN for chamber experiments. The red markers represent measurement data and the black markers represent model results.

3.2 Isomer distribution for IN during SOAS

The 0D model was used to estimate the relative abundance of IN isomers during the SOAS study. The diurnal average of isoprene, OH, NO, NO_2, O_3 and HO_2 were calculated and the 0D model was used to simulate the relative concentrations of the IN isomers as they were produced from isoprene oxidation and lost to OH, O_3 and deposition throughout the day. The reaction was initiated at 6:00 AM (reaction time equals 0) and the duration was 24 hours. The simulated IN isomer composition is shown in Figure S8. A diurnal isomer-weighted IN sensitivity was calculated based on the simulated IN isomer distribution (Figure S9). The same diurnal calibration factors were applied to interpret IN raw data for each individual day.
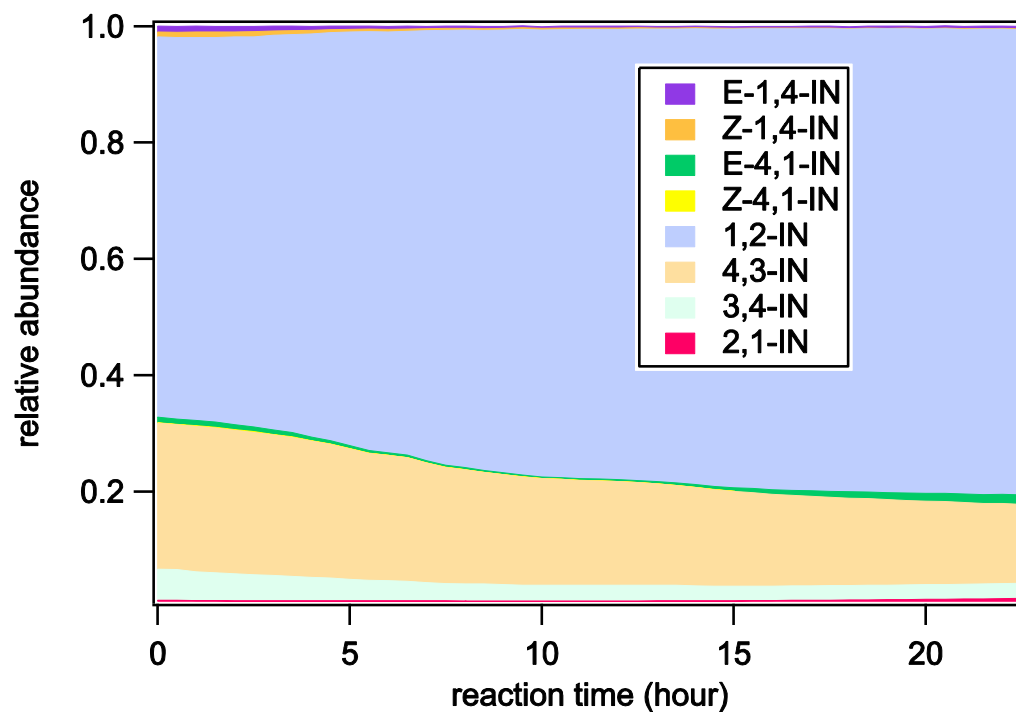
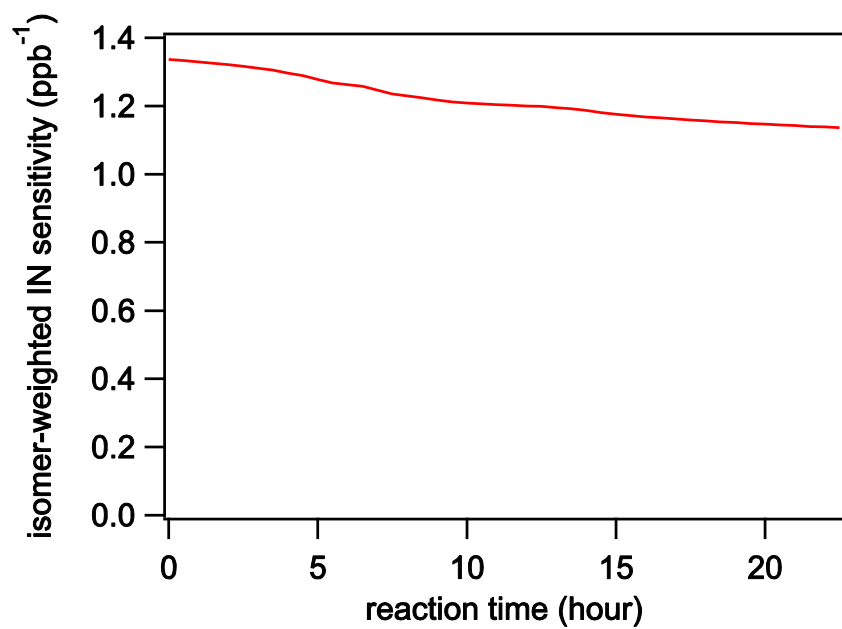Figure S8. Simulated diurnal IN isomer distribution during SOAS.

Figure S9. The diurnal isomer-weighted IN sensitivity during SOAS

4 Isoprene RO₂ distribution and RO₂ lifetime

During SOAS, the RO$_2$ loss rates to NO and HO$_2$ are slow, compared with 1,6-H shift rate constant for the cis-δ-RO$_2$. As a result, the yield of total RO$_2$ from OH addition to isoprene, defined as the amount of RO$_2$ produced relative to the amount of isoprene consumed, can decrease with RO$_2$ lifetime, as *cis*-δ-RO$_2$ radicals isomerize into hydroperoxy aldehyde (HPALD) and other RO$_2$ covert to *cis*-δ-RO$_2$ through O$_2$ loss and addition (Peeters et al., 2014). The yield of the products with respect to RO$_2$ lifetime was calculated with the Kintecus software, and the result is shown in Figure S10. The *cis*-δ-RO$_2$ radicals become less important with longer RO$_2$ lifetime. Besides RO$_2$ and HPALD, OH addition to isoprene also forms a stable carbonyl product, with a yield of 2% (Fan and Zhang, 2004; Peeters et al., 2014). The daytime total RO$_2$ loss rate to NO and HO$_2$ was on the order of 0.05 s^{-1}, so the RO$_2$ yield at 20 s was chosen to calculate the IN production rate during SOAS. With an RO$_2$ lifetime of 20 s, the isoprene oxidation products consist of 83% RO$_2$, 15% HPALD and 2% carbonyl product. The 83% RO$_2$ products include 1% *cis*-δ-RO$_2$, 2% *trans*-δ-RO$_2$ and 81% β-RO$_2$.
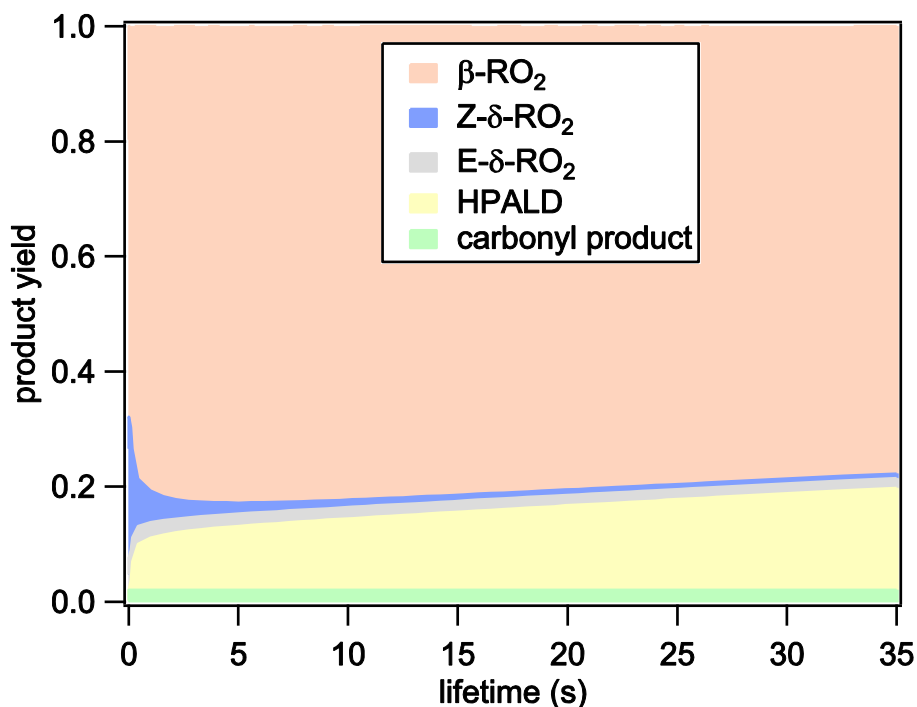

Figure S10. Product yield from OH addition to isoprene.

5   Sensitivity tests on LIM1 mechanism

The uncertainties in kinetics data for RO_2 interconversion and 1,6-H shift can cause error in the isoprene RO_2 and IN isomeric distribution. For the LIM1 mechains, the uncertainties for the equlibrium constants $K_{eq}=k(+O_2)/k(-O_2)$ are a factor of 1.5, and the uncertainties for the 1,6-H shift rate constants $k_{1,6-H}$ are a factor of 2.4 (Peeters et al., 2014). Sensitivity tests were performed by varying the rate constants $k(+O_2)$ (or $k(-O_2)$) by 1.5 times and $k_{1,6-H}$ by 2.4 times, and calculating the relative abundance of the RO_2 isomers. We found changing $k_{1,6-H}$ had no influence on the relative abundance of RO_2 isomers, although it significantly influences the yield of HPALD. Changing $k(+O_2)$ or $k(-O_2)$ only affected the production rate of total RO_2, but had no ifluence on the relative abundance of RO_2 isomers. The isomeric distribution was affected most when $k(+O_2)$ or $k(-O_2)$ were varied differently for β-RO_2 and for δ-RO_2. When $k(+O_2)$ values for δ-RO_2 were increased by 1.5 times and $k(-O_2)$ values for β-RO_2 were decreased by 1.5 times, the yield of 1,2-RO_2 and 4,3-RO_2 became 32% and 17% repectively, which will lead to a total MVK+MACR yield of 49%. This is significantly lower than the experimental MVK+MACR yield from isoprene high NO oxidation (Liu et al., 2013; Park et al., 2004). When $k(+O_2)$ values for δ-RO_2 were increased by 1.5 times and $k(-O_2)$ values for β-RO_2 were kept as orignial, the yield of 1,2-RO_2 and 4,3-RO_2 were 37% and 19%, more consistent with the experimental MVK+MACR yield. This set of RO_2 isomer distribution was treated as the high δ-RO_2 senario. When $k(+O_2)$ values for δ-RO_2 were decreased by 1.5 times and $k(-O_2)$ values for β-RO_2 were increased by 1.5 times, the yield of 1,2-RO_2 and 4,3-RO_2 became 50% and 26%, and the combined MVK+MACR yield of 76% was still within the uncertainty reported by experimental studies.This set of RO_2 isomer distribution was treated as the high β-RO_2 scenario. The three set of isomer distributions, base scenario, high δ-RO_2 senario and high β-RO_2 scenario were used to estimate the uncertainty associated with the LIM1 mechanism. The total error in RO_2 distribution is 20%, calculated as the weighted relative error of each RO_2 isomer.

Table S2. Deviation of RO_2 isomer distrubtion due to error in RO_2 interconversion rate constants.

RO_2 isomer	Z-1,4	1,2	E-1,4	Z-4,1	4,3	E-4,1	3,4	2,1
Base	0.16	0.43	0.04	0.07	0.23	0.01	0.04	0.01
high δ-RO_2	0.19	0.39	0.06	0.09	0.20	0.02	0.04	0.01
high β-RO_2	0.10	0.51	0.02	0.04	0.27	0.01	0.04	0.01

6   4,3-IN sensitivity and sample humidity

The stability of the CIMS signal for 4,3-IN under different humidity was investigated with the setup in Figure S11a. A gas flow that contained constant 4,3-IN concentration and varying humidity was sampled by the CIMS. The constant 4,3-IN gas flow was generated by bubbling N_2 through a 4,3-IN solution kept at 0 °C. The IN signal normalized to the signal of the reagent ion was stable with varying sample humidity (Figure S11b). CIMS was configured with constant water vapor addition to the analyte compounds downstream the orifice.
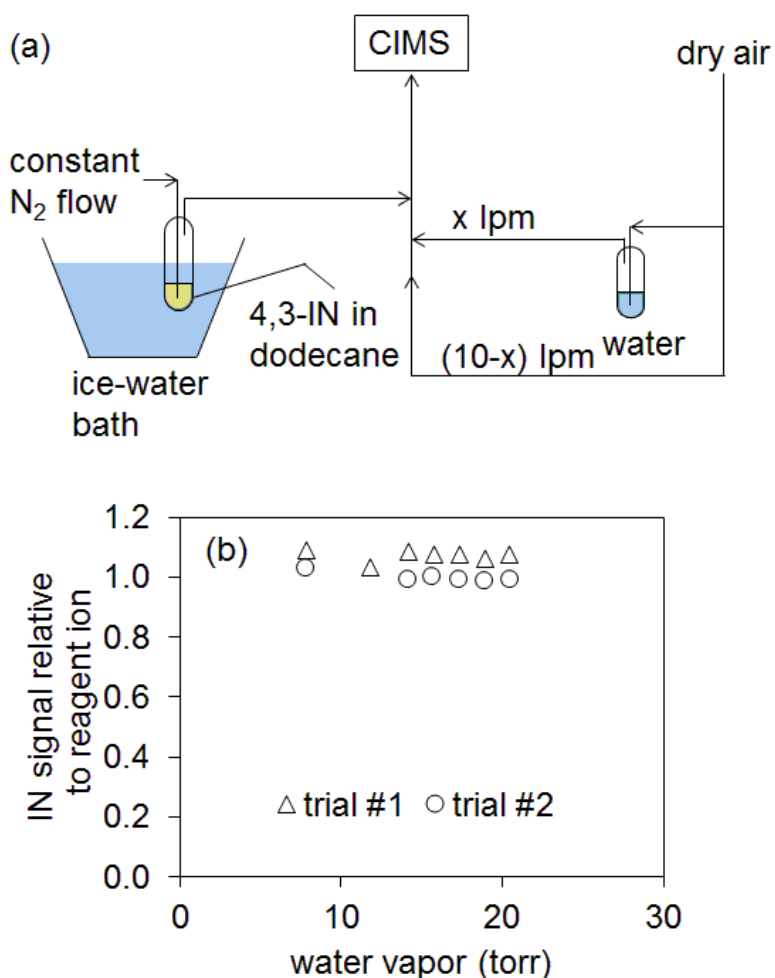

Figure S11. (a) Experimental setup for the CIMS humidity test. (b) Relative CIMS signal for 4,3-IN with varying sample humidity.

7   The influence of downward mixing on morning [IN] increase

The rate at which [IN]/([MVK]+[MACR]) increased can be described using the following expression.

$$\text{rate} = \frac{d^{[IN]}/_{[MVK]+[MACR]}}{dt} \tag{5}$$

If we define rate as variable r, the concentration of IN as x and the concentration of MVK+MACR as y, we will have the following expression.

$$r = \frac{d^{x}/_{y}}{dt} \tag{6}$$

Since the concentration of IN (x) and the concentration of MVK+MACR (y) both changed with time. Equation (6) can be written as the following.

$$r = -\frac{x}{y^2}\frac{dy}{dt} + \frac{1}{y}\frac{dx}{dt} \tag{7}$$

In Equation (7), dy/dt is the growth rate of MVK+MACR, and dx/dt is the growth rate of IN.

The 2-hour period from 7:00 AM to 9:00 AM for the 12-day average was chosen as the time window to estimate the contribution of downward mixing. To simplify the calculation, the average changing rate was used for IN and MVK+MACR, instead of the instantanous rate. That modifies Equation (7) to the form of Equation (8) below.

$$r = -\frac{\bar{x}}{\bar{y}^2}\frac{\Delta y}{\Delta t} + \frac{1}{\bar{y}}\frac{\Delta x}{\Delta t} \tag{8}$$

$\bar{x}$ and $\bar{y}$ are the average concentrations of IN and MVK+MACR between 7:00 AM and 9:00 AM. The growth rate of the [IN]/([MVK]+[MACR]) ratio was controlled by the growth rate of MVK+MACR and the growth rate of IN. The growth rate of the [IN]/([MVK]+[MACR]) ratio for measurement data r_{obs} was higher than the growth rate of the [IN]/([MVK]+[MACR]) ratio for simulated results r_{mod} (Figure S13a and S13b). The growth rate of [MVK]+[MACR] was less likely to be affected by downward mixing, because significant amount of MVK+MACR was produced at night through isoprene ozonolysis. Therefore here we assume the difference between r_{obs} and r_{mod} was caused only by the difference in $\Delta x/\Delta y$, which is the growth of [IN].

The growth rate of [IN] can be calculated from Equation (9). Using r_{mod} in Equation (9) we can calculate the the [IN] growth rate caused only by isoprene photochemistry in the current day.

Using r_{obs} in Equation (9), we can calculate the total [IN] growth rate, which is the sum of isoprene photochemistry and IN downward mixing. $\bar{x}$ and $\bar{y}$ are average [IN] and [MVK]+[MACR] based on observation. When r_{obs} is used in Equation (9), $\bar{x}$ based on modeling should be used. However, the 0D model cannot simulate absolution IN concentration, so observed average [IN] was used instead, which will make the result slightly biased high.

$$\frac{\Delta x}{\Delta t} = \bar{y}(r + \frac{\bar{x}}{\bar{y}^2}\frac{\Delta y}{\Delta t}) \tag{9}$$

The calculated total [IN] growth rate with r_{obs} is 9.93×10^{-3} ppt/s, which is consistent with the [IN] growth rate derived directly from IN measurement (Figure S13d). When r_{mod} was applied in Equation (9), we could calculate [IN] growth caused by isoprene chemistry to be 5.65×10^{-3} ppt/s, 7.28×10^{-3} ppt/s and 8.98×10^{-3} ppt/s, for IN yield of 6%, 9% and 12%. The difference between total [IN] growth rate and [IN] growth rate caused by photochemistry was attributed to downward mixing. On average, the influence of downward mixing was estimated to be 27($\pm$16)%.

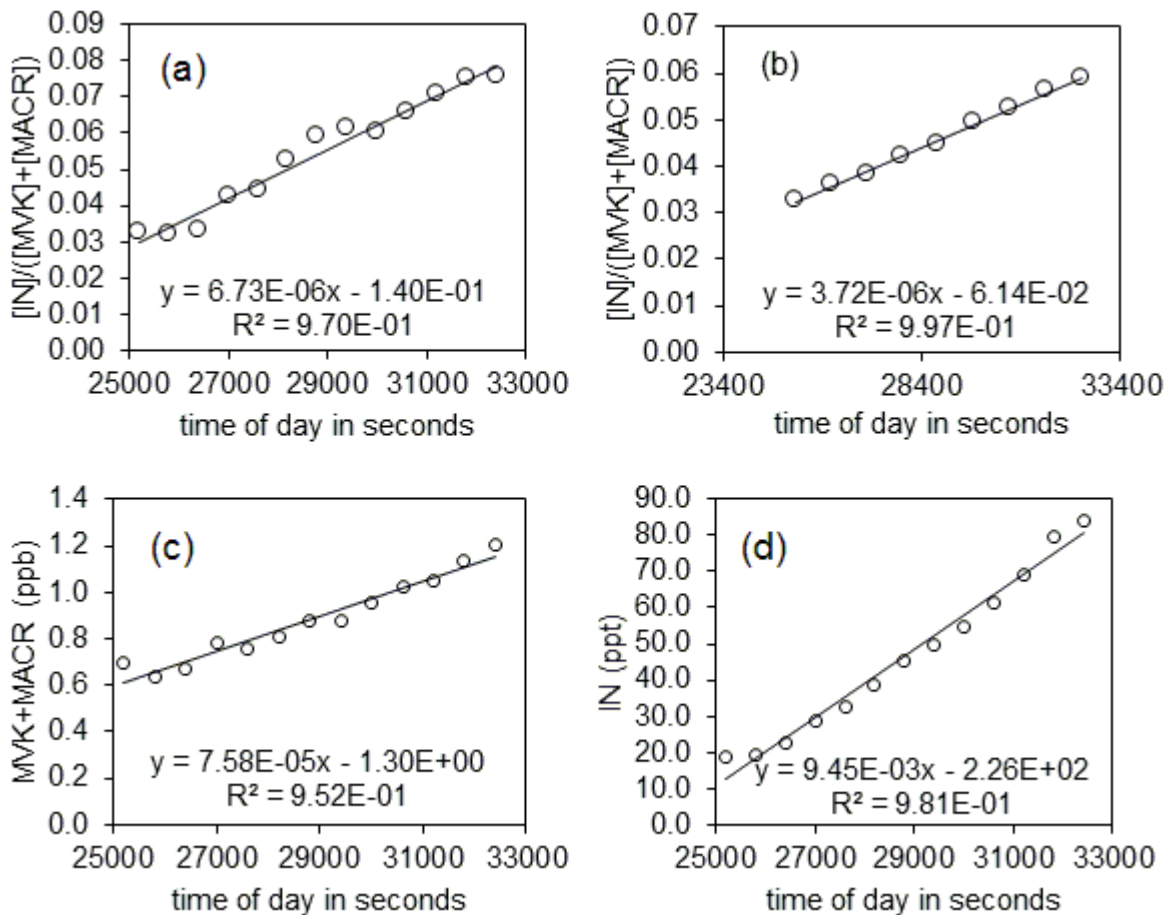Figure S12. Growth rate of the (a) observed and (b) simulated [IN]/([MVK]+[MACR]) ratio. The simulated ratio is derived with a 9% IN yield in the model. (c) Growth rate of observed MVK+MACR concentration. (d) Growth rate of observed IN concentration.

References

Fan, J., and Zhang, R.: Atmospheric Oxidation Mechanism of Isoprene, Environmental Chemistry, 1, 140, 10.1071/en04045, 2004.

Liu, Y. J., Herdlinger-Blatt, I., McKinney, K. A., and Martin, S. T.: Production of methyl vinyl ketone and methacrolein via the hydroperoxyl pathway of isoprene oxidation, Atmospheric Chemistry and Physics, 13, 5715-5730, 10.5194/acp-13-5715-2013, 2013.

Park, J., Jongsma, C. G., Zhang, R., and North, S. W.: OH/OD Initiated Oxidation of Isoprene in the Presence of O2 and NO, The Journal of Physical Chemistry A, 108, 10688-10697, 10.1021/jp040421t, 2004.

Peeters, J., Müller, J.-F., Stavrakou, T., and Nguyen, V. S.: Hydroxyl Radical Recycling in Isoprene Oxidation Driven by Hydrogen Bonding and Hydrogen Tunneling: The Upgraded LIM1 Mechanism, The Journal of Physical Chemistry A, 118, 8625-8643, 10.1021/jp5033146, 2014.